DOI: 10.13009/EUCASS2017-499

Comparison of high speed PIV experiments, unsteady pressure measurements and DES computations of a transonic Ariane 5 base-flow using POD

F. Schrijer, T. Horchler**, M. Fertig**, S. Deck***, K. Hanneman** and P. van Gent**
TU Delft, The Netherlands; ** DLR, Germany; * ONERA, France*

Abstract
The present work is conducted in the framework of the ESA TRP "Launcher Base Flows and Shock Interactions Regions Improved Load Characterization", where high speed PIV measurements and unsteady pressure measurements performed in the DNW-HST on a 1:60 scale Ariane 5 are compared to simulations using IDDES and ZDES for the same configuration and flow conditions. The goal of the investigation is to identify how well the computations are capable of predicting the salient features of the transonic buffeting phenomenon. In order to make a valid comparison, it is confirmed that both the experimental as well as the numerical data is properly converged in order to extract flow statistics. It is found that due to the spatial filtering inherent to the PIV processing the measured velocity fluctuations are modulated. Furthermore a POD analysis shows that both the numerics and the experiments return the same modes (both for velocity field and pressure distribution) which indicates that both approaches contain similar large scale flow dynamics.

1. Introduction

During the ascent of the Ariane 5 launch vehicle significant dynamic loads on the nozzle can cause deformations which may lead to catastrophic failure of the engine. This phenomenon is known as base buffeting and is caused by a strong flow separation at the base of the launcher vehicle. Wind tunnel experiments and CFD investigations have been conducted to gain more insight into this phenomenon, to improve modeling and to assess mitigation strategies (see, e.g., [1], [2]). Compared to experiments, CFD computations typically achieve a much higher spatial and temporal resolution but span a shorter time period and may not capture all flow features correctly. In experiments on the other hand, it is easy to achieve long time series but high sampling frequencies are difficult to realize. Furthermore, the experimental measurement chain introduces spatial and temporal filtering (modulation) that damps any frequencies above a certain threshold and leaves all flow scales smaller than a certain size unresolved. Given these merits and drawbacks of both types of investigations, comparing the outcome of experiments and simulations is essential for the proper interpretation and mutual validation of their results.

Experimental and CFD results are often only compared in terms of mean and fluctuating surface pressure data and velocity fields. Although these comparisons are very instructive regarding the statistical properties of the flow field, they do not directly provide any information about the underlying flow dynamics. Alternatively, velocity and pressure (cross) spectra may be compared but the comparison may suffer from the resolution issues and sampling duration mentioned before. Meanwhile, methods for data decomposition like proper orthogonal decomposition (POD) have shown potential in analyzing experimental and numerical results. The method isolates dominant flow modes which may be used to construct low-order models of the flow. The method relies on the availability of suitable input data only and does not require making any assumptions about the flow. POD [3] is a well established analysis tool in the fluid dynamics community. Using snapshots with spatially resolved data, it yields spatial modes on an orthogonal basis ranked by energy content.

The present work investigates the suitability of using POD to compare experimental and numerical results. The study compares numerical and experimental datasets of the flow over the nozzle of the Ariane 5. The experimental data consists of unsteady pressure measurements in conjunction with high speed planar PIV measurements. These results were obtained in the framework of the ESA TRP `Unsteady Subscale Force Measurements Within a Launch Vehicle Base Buffeting Environment'. The numerical data was obtained by detached-eddy simulations (IDDES and ZDES) in the follow-up ESA TRP `Base Flows and Shock Interaction Regions Improved Load Characterization' [4].

DOI: 10.13009/EUCASS2017-499

2. Database description

The experiments were conducted in the DNW-HST on a 1:60 Ariane 5 model. The free stream flow conditions were Mach 0.8 and the unit Reynolds number was $Re_m = 12.8 \times 10^6$ m^{-1}. Velocity measurements were performed using particle image velocimetry (PIV). The field of view was situated in the no booster plane encompassing the nozzle of the centre stage of the launcher. The experiments were performed at an acquisition frequency of 2.7 kHz and the PIV snapshots were processed with a window size of 32 x 32 pixels with 75% overlap which resulted in a spatial resolution of 3 mm. In addition the model was instrumented with 144 Kulite sensors to measure the unsteady pressure signal at a frequency of 12.8 kHz. See [2] for more details.

Furthermore numerical flow simulations were done using IDDES using the DLR TAU code [5] and ZDES [6] approaches on the same geometry (including wind tunnel model support) and free stream flow conditions. For the IDDES computations were conducted on an hybrid mesh consisting of 22 x 10^6 points with a physical time step of 2 μs. During post-processing the flow field was down sampled at frequency of 50 kHz for a total (physical) duration of 163.5 ms (equivalent to 192 shedding cycles for $St_D = 0.4$). For the ZDES computations a structured mesh was used having 75 x 10^6 cells and a physical time step of 1 μs, in this case the flow was subsampled at 250 kHz for a duration of 240 ms (281 shedding cycles). The typical spatial resolution for the CFD simulations was much better than the PIV experiments (typically smaller than 1 mm).

Table 1: Unsteady pressure database

	Kulites	IDDES	ZDES
Sampling frequency [kHz]	12.8	50	250
# samples	131076	8174	60000
Total duration [ms]	10240	163.5	240

Table 2:Velocity database

	PIV	IDDES
Sampling frequency [kHz]	2.7	50
# samples	2728	8174
Simulation duration [ms]	1010	163.5
Maximum Str_D	0.45	8.33
Minimum Str_D	3.3×10^{-4}	2.0×10^{-3}
Data points	13984	24375
Spatial resolution [mm]	3	<<1

3. Flow field statistics

For the PIV measurements and IDDES computations convergence study was carried out to verify that the flow statistics are converged (values below 1%). Since the PIV measurements were acquired at 2.7 kHz, the measurements were basically uncorrelated in time and sufficient samples are available, 1500 samples were needed for convergence. For the IDDES computations it was found that approximately 4000 samples were needed. This difference is explained by the fact that the IDDES samples are correlated in time. Using autocorrelation analysis this was indeed verified and it was established that subsampling to 5 kHz was needed to obtain uncorrelated samples. Figure 1 shows the comparison between the IDDES computations and PIV measurement for the mean horizontal velocity component. It can be seen that the overall flow fields match well in terms of velocity magnitude, shear layer development and reattachment location.

DOI: 10.13009/EUCASS2017-499

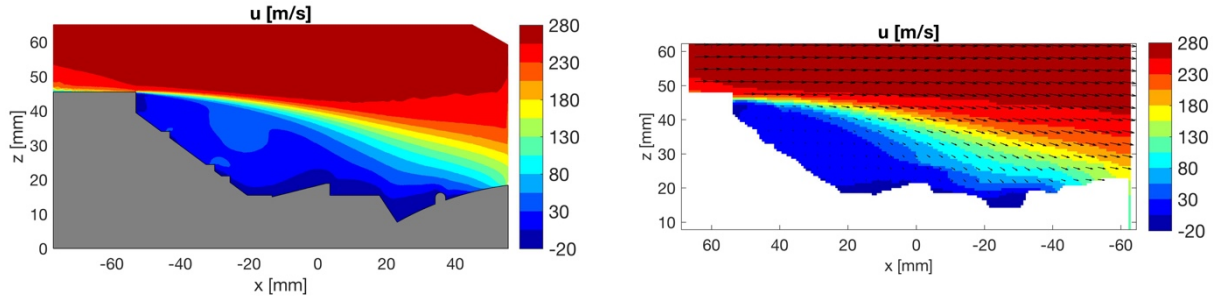

Figure 1: Average flow field IDDES (left) and PIV (right)

Figure 2 shows the total velocity fluctuations, as expected maximum values are found in the shear layer and near the reattachment location. When comparing the fluctuations it is clear that PIV under predicts the magnitude with approximately 30%. This can be ascribed to the fact that the PIV cross-correlation approach averages the local velocity in a moving average sense where the equivalent kernel size of the moving average filter is between 0.5 – 1 times the interrogation window size (WS), [7].

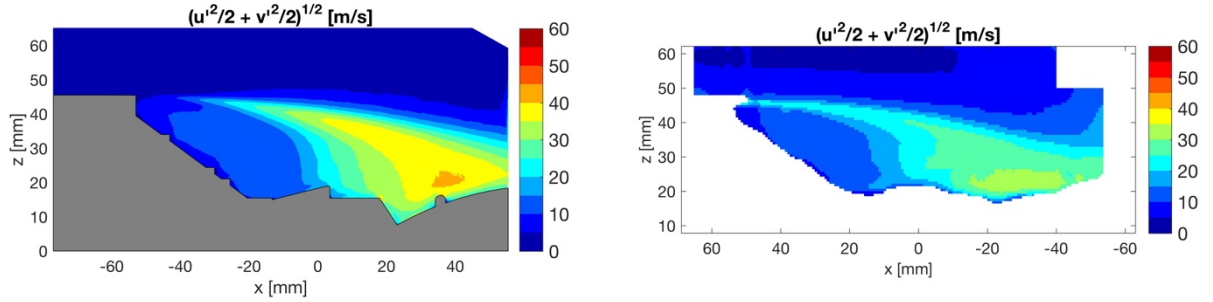

Figure 2: Total rms velocity fluctuations IDDES (left) and PIV (right)

In order to verify this effect, the IDDES snapshots have been filtered by applying a moving average filter equal to 1.8 mm (0.5 WS) and 3.6 mm (1 WS), see Figure 3. It is clear that the overall fluctuations are reduced when the filter strength (larger kernel size) increases. For a kernel size of 3.6 mm the results compare very well to those from PIV.

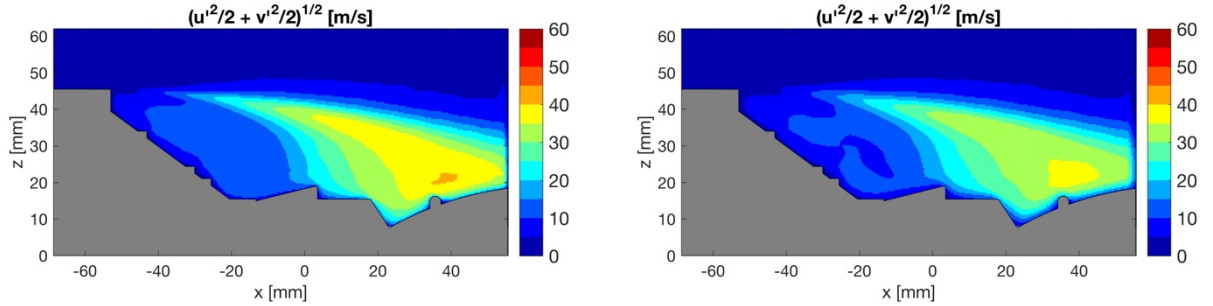

Figure 3: Total rms velocity fluctuations for moving average filtered IDDES data kernel size 1.8 mm (left) and 3.6 mm (right)

DOI: 10.13009/EUCASS2017-499

4. POD analysis

4.1 Velocity POD analysis

In order to further compare the dynamical flow features returned by the simulations and experiments a POD analysis is conducted. The benefit of using POD is that the approach relies on a dataset that contains preferably uncorrelated samples, therefore making the difference in acquisition frequencies between the measurements and simulations of minor importance. The POD approach gives an energy ranked decomposition of a velocity field u(**x**,t):

$$u(\boldsymbol{x},t) = \bar{u}(\boldsymbol{x}) + u'(x,t) = \bar{u}(\boldsymbol{x}) + \sum_{n=1}^{N} c_n(t)\sqrt{\lambda_n}\varphi_n(\boldsymbol{x})$$

where **x** is the spatial coordinate, t is the temporal coordinate, U is the mean velocity and u' is the fluctuating velocity component. The basis functions $\boldsymbol{\phi}_n$ are normalized and spatially orthogonal. The POD modes are obtained as the eigenmodes of the autocorrelation matrix **R**:

$$\boldsymbol{R}\varphi_n = \lambda_n\varphi_n \text{ where } R_{ij} = \overline{u'(\boldsymbol{x}_\iota,t)u'(\boldsymbol{x}_J,t)}$$

Since the basis functions are normalized, the eigenvalue λ_i represents the contribution of the POD mode to the total fluctuating energy:

$$\langle\overline{u'(\boldsymbol{x}_\iota,t)u'(\boldsymbol{x}_J,t)}\rangle = \sum_{n=1}^{N}\lambda_n.$$

In the POD analysis it is common to sort the mode in order of decreasing eigenvalues (energy) i.e. importance, so that the dominant modes can be easily identified.

For more information on the implementation and mathematical background of POD the reader is referred to [3].

The POD application described above (method of snapshots) is a purely statistical operator and does not use any of the temporal information that is contained in the data. In fact, the method shows fastest convergence when the individual snapshots are uncorrelated in time as was already referred to before. Here the method of snapshots is used to identify the most energetic structures of the turbulent separated flow field.

According to the above outlined procedure the POD modes are computed for the PIV measurements. For completeness also here a convergence study is performed to assess whether the results are statistically significant and thus do not depend anymore on the sample size. First the so-called POD spectrum is inspected for various sample sizes, see Figure 4 - left. It appears that for sample sizes larger than 1000 the spectrum is identical and independent of the sample size. This also confirms that the amount of PIV velocity snapshots (2728) is sufficient in order to perform a POD analysis. A similar procedure has been carried out for the IDDES computations. In this case various sample sizes have been evaluated with and without skip (subsampling the dataset). Figure 4 – right shows the different POD spectra and it can be concluded that at least 500 samples are needed with a skip of 10 (subsampling at 5 kHz) to achieve a converged spectrum (the results for 500 or 700 samples at 5 kHz are nearly identical).

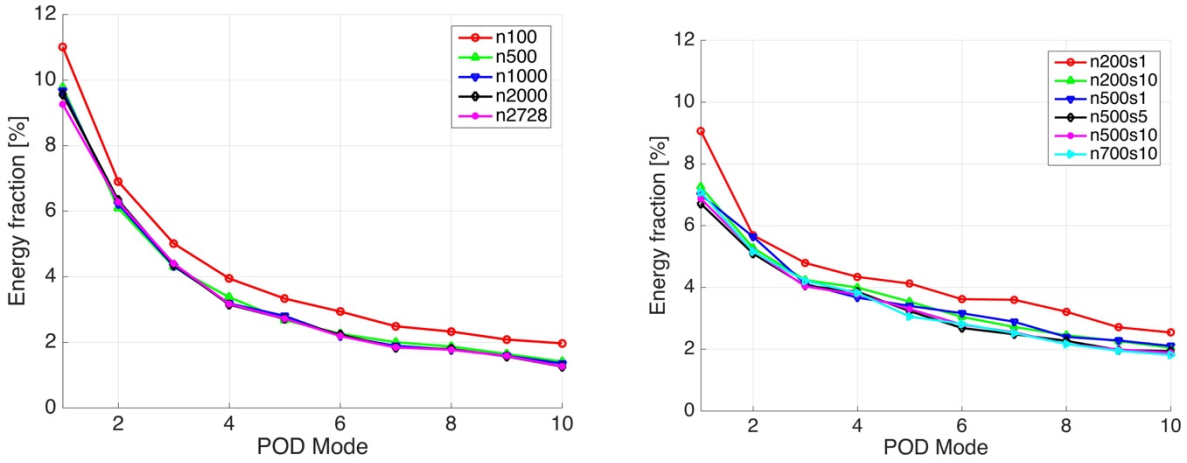

Figure 4: POD spectrum for various sample sizes (value behind n) indicated by n for PIV (left) and IDDES (right). The number behind s indicates number of snapshots that were skipped (amount of subsampling).

DOI: 10.13009/EUCASS2017-499

When comparing the POD spectra it can be seen that the first couple of modes contain more energy for the PIV measurements. This can be attributed to the fact that the small scales are filtered out by the PIV processing and thus are not represented by POD modes. However the IDDES has more scales, leading to a more flatter POD spectrum.

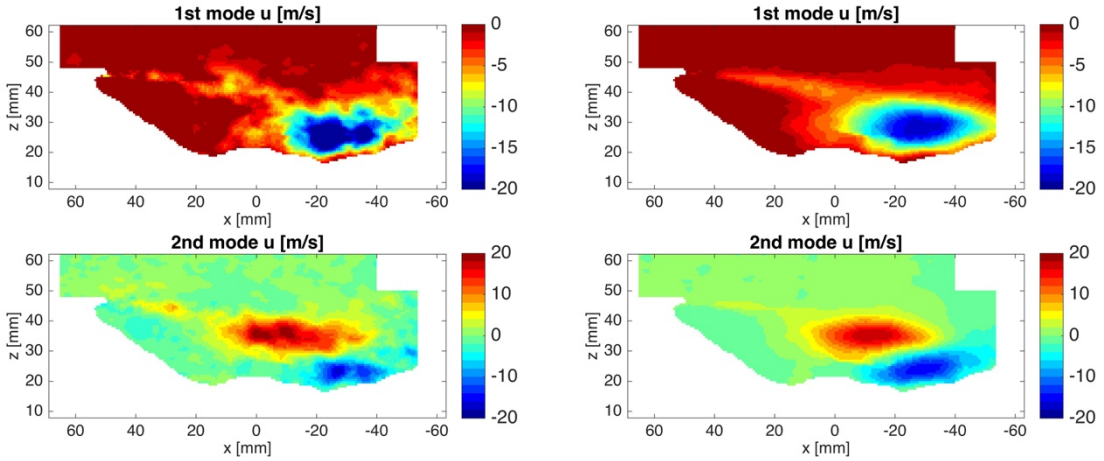

Figure 5: 1st and 2nd POD mode of PIV results for 100 (left) and 2728 (right) snapshots

In Figure 5 the 1st and 2nd POD modes are compared for 100 and 2728 samples. Although the result for only 100 samples looks rather coarse (not fully converged), it already contains essentially the same modal information as for the complete dataset. The modes look similar to those found for a classical axisymmetric backward facing step where mode 1 represents the pulsation of the recirculation bubble while mode 2 represents the undulating motion of the shear layer [8].

The POD modes for various sample sizes are also assessed for the IDDES computations. Two cases are shown in Figure 6, both are subsampled to 5 kHz. The result for a sample size of 200 is not yet converged, when compared to the result for 700 snapshots. From these results however it appears that the 1st mode is already better converged compared to the 2nd mode (and higher modes), which is expected considering that it contain more energy. In addition the results for 500 snapshots were compared to those of 700 and the results were essentially the same with a difference of less than 1%, from which it can be concluded that the amount samples are enough to get well converged POD results.

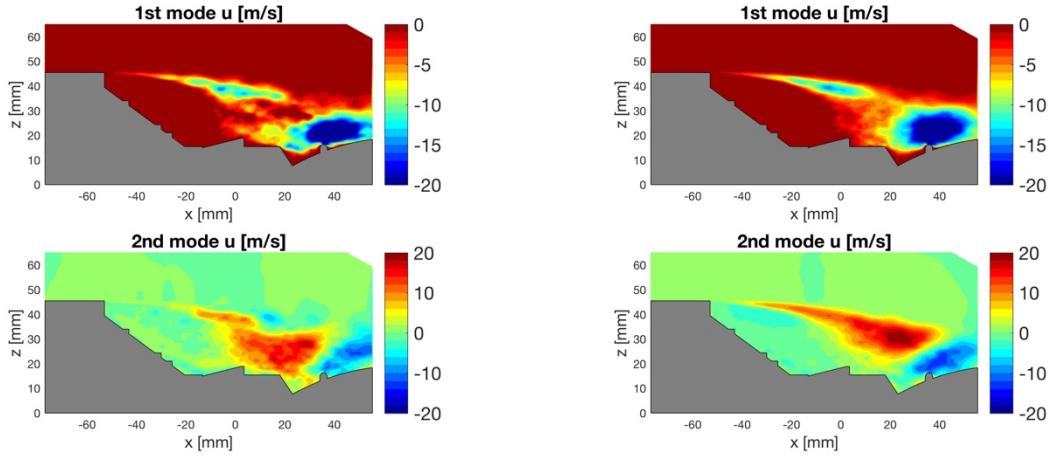

Figure 6: 1st and 2nd POD mode of IDDES results for 200 (left) and 700 samples (right), subsampled at 5 kHz

In order to compare the POD modes from PIV to those from the IDDES computations, both modes are plotted side by side in Figure 7. As can be seen, the modes are very similar. However modes 3 and 4 seem to be swapped: mode 3 from PIV looks similar to mode 4 from IDDES and mode 4 from PIV looks similar to mode 3 from IDDES. This aspect is not unexpected since the ordering of the modes is done based on the energy content and for modes 3 and 4 the spectrum is already rather flat (see Figure 4) such that a mode reversal can easily happen. In both cases the 1st mode represents the pulsation of the separated region, while modes 2 and 3 represent the shear layer undulation.

DOI: 10.13009/EUCASS2017-499

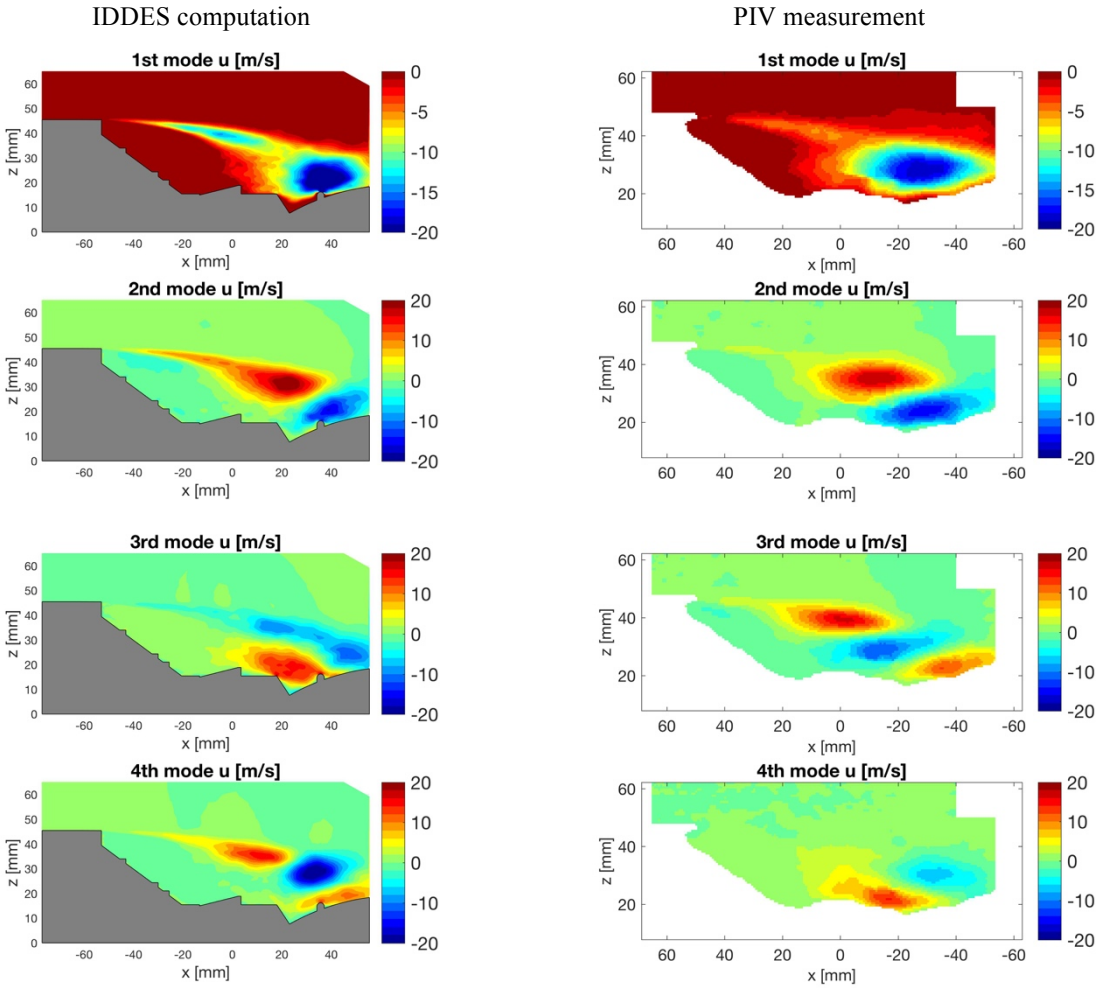

Figure 7: Comparison of POD modes from IDDES (left) and PIV (right)

In order to quantify the similarity of the modes the cross-correlation coefficient between the PIV and IDDES POD modes is computed according to:

$$\rho_n = (\varphi_n)_{piv} \otimes (\varphi_n)_{IDDES}$$

For various sample sizes and skip values (subsampling factors) the maximum cross-correlation coefficients are reported in Table 1. As can be seen from the table, the correlation coefficient increases (for well converged values) up to values between 0.9 and 0.7 indicating the good correspondence between the numerical and experimental results.

Table 3: Maximum cross-correlation coefficient between PIV and IDDES POD modes

ρ_k	Mode 1	Mode 2	Mode 3	Mode 4
n200s1	0.62	0.51	0.50	0.43
n500s1	0.75	0.47	0.60	0.57
n200s10	0.82	0.63	0.41	0.54
n500s10	0.88	0.78	0.58	0.67
n700s10	0.89	0.84	0.71	0.81

DOI: 10.13009/EUCASS2017-499

4.2 Unsteady pressure POD analysis

In addition to the POD analysis on the velocity data, a similar analysis is performed for the pressure data. For this comparison the IDDES data are used in combination with ONERA ZDES data and experimental data obtained using the Kulite sensors. Since the IDDES data was available on the full computational grid it hase been interpolated to the ring positions where the sensors were located (but still oversampled in the circumferential direction) which is indicated by 'IDDES full' and to the sensor locations indicated by 'IDDES sensor'. Since for the ONERA ZDES computations only the data was available at the sensor locations, the results only include 'ONERA sensor'.

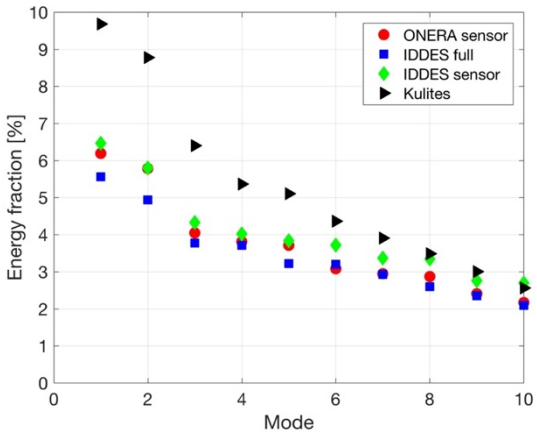

Figure 8: POD spectra for the pressure data

Figure 8 shows the POD spectra for the various data sets. The IDDES sensor and ONERA sensor spectra are very similar while the IDDES full is lower. The Kulites data consistently have higher values for low mode numbers, however at higher modes (> 7) the energy content becomes similar.

DOI: 10.13009/EUCASS2017-499

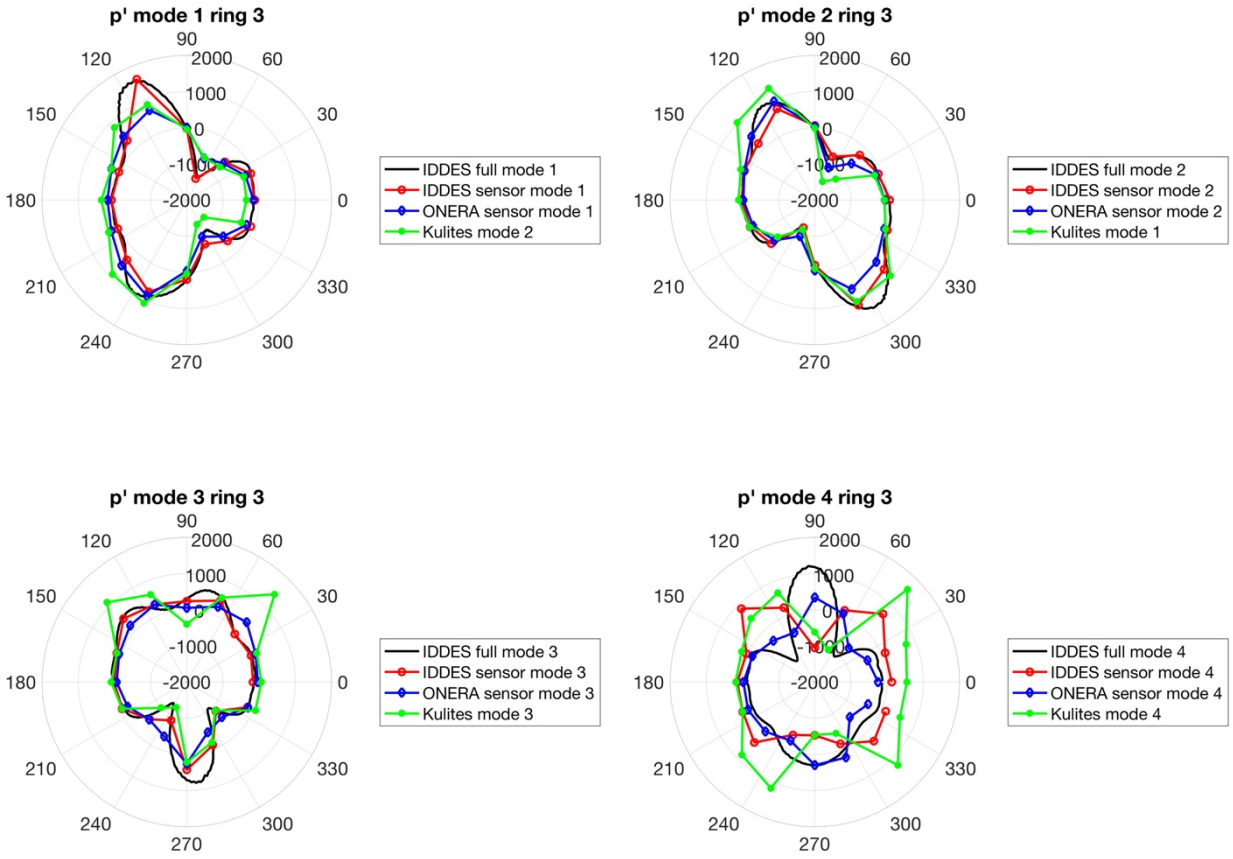

Figure 9: Comparison of the first 4 pressure POD modes for ring 3

The first 4 POD modes are shown in Figure 9, the modes are plotted for ring 3 since the results for ring 1 and 2 and 5 are very similar. The contributions of 6 – 11 is nearly negligible.
Mode 1 represents the anti-symmetric (side-load enforcing) mode. For the Kulites this mode shows up as mode 2 but is plotted together with mode 1 of the computations because it represents the same dynamics. Mode 2 represents the symmetric (ovalization) mode (and for the Kulites this is mode 1). For these modes the agreement between computations and experiments is very good. For higher modes there is still an agreement but the similarities are less striking.

DOI: 10.13009/EUCASS2017-499

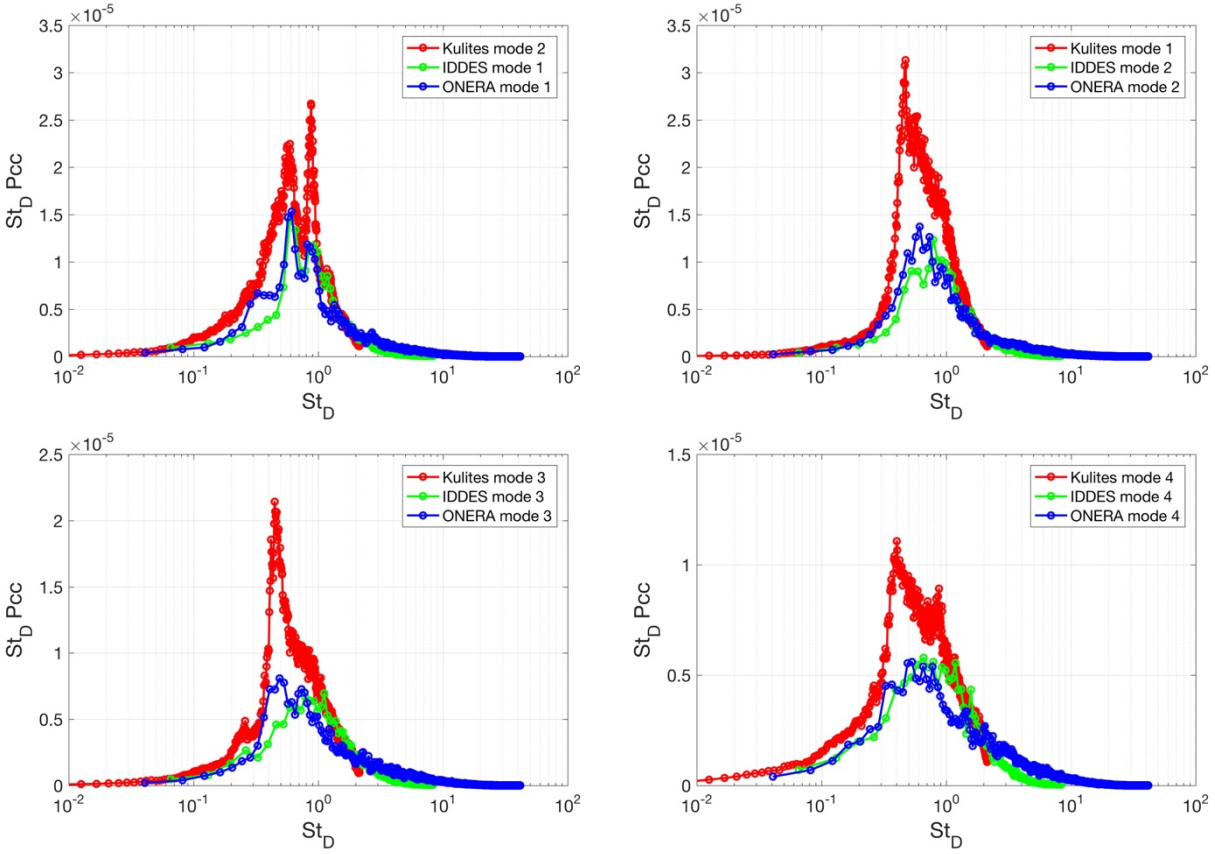

Figure 10: Comparison of the pre-multiplied power spectrum of the mode time coefficients

The power spectrum of the POD time coefficients is shown in Figure 10 per mode and compared for all datasets. For all modes the magnitude of the power spectrum is the highest for the experimental data. When looking in more detail at the anti-symmetric (mode 1), it can be seen that all datasets show a peak between $St_D = 0.5 – 0.6$ and a second one around $St_D = 0.8$. For the symmetric mode (mode 2) no clear peaks can be observed for the computations. For the IDDES data the overall spectrum has a maximum around $St_D = 0.6$ while for the ONERA ZDES data it lies around a slightly higher Strouhal number $St_D = 0.7$. The maximum of the experimental data is found at $St_D = 0.4$.

5. Conclusions and recommendations

The flow in the base region of the Ariane 5 launcher is investigated both experimentally and computationally. The velocity field in the no-booster plane is measured by means of particle image velocimetry and additionally unsteady pressure measurements are performed using 144 Kulite sensors. The computational simulations are performed using unsteady detached eddy simulations using IDDES (DLR Tau code) and ZDES (ONERA). It is confirmed that the results are properly converged for both the PIV data (minimum of 1500 samples needed) and the IDDES computations (minimum of 4000 samples needed). Furthermore it is established that for the IDDES data a subsampling is needed to 5 kHz in order to get uncorrelated data such as to get best convergence for flow statistics. The flow field statistics for PIV and IDDES are similar provided that the IDDES data is moving averaged filtered in order to mimic the PIV data processing procedure. The POD modes for both the IDDES and PIV dataset are very similar. The similarity is quantified by cross-correlating the modes and values ranging between 0.9 (for the most energetic modes) and 0.7 (higher order modes) are found. The pressure POD modes showed good agreement between DLR – IDDES computations, ONERA –ZDES computations and Kulite measurements. The magnitude of the power spectrum of the time-coefficients for the experiments were larger compared to the computational results but the overall distribution was similar.

DOI: 10.13009/EUCASS2017-499

Acknowledgements

The present research was performed in the framework of the ESA TRP “Base Flows and Shock Interaction Regions Improved Load Characterization”.

References

[1] K. Hannemann, J. Pallegoix, M. Frey, S. Deck, H. Maseland, F. Schrijer, H. Lambare and R. Schwane, “Launch vehicle base buffeting – recent experimental and numerical investigation,” in *Proceedings of the 7th European Symposium on Aerothermodynamics for Space Vehicles (SP-692)*, edited by L. Ouwehand (Spacebooks Online, 2011)

[2] F. Schrijer, A. Sciacchitano, F. Scarano, K., Hannemann, J. Pallegoix, R. Schwane and H. Maseland, “Experimental Investigation of Base Flow Buffeting on the Ariane 5 Launcher using high Speed PIV”, in *Proceedings of the 7th European Symposium on Aerothermodynamics for Space Vehicles (SP-692)*, edited by L. Ouwehand (Spacebooks Online, 2011)

[3] G. Berkooz, P. Holmes and J. L. Lumley, “The proper orthogonal decomposition in the analysis of turbulent flows”, Annu. Rev. Fluid Mech. 25: 539-75 (1993)

[4] Heinrich Lüdeke, Jean Daniel Mulot, and Klaus Hannemann. "Launch Vehicle Base Flow Analysis Using Improved Delayed Detached-Eddy Simulation", AIAA Journal, Vol. 53, No. 9 (2015), pp. 2454-2471.

[5] Schwamborn D., Gerhold T. and Heinrich R. (2006) The DLR-TAU-Code: Recent Applications in Research and Industry. European Conference on Computational Fluid Dynamics, ECCOMAS CFD.

[6] Deck, S., Zonal Detached Eddy Simulation of the Flow around a High-Lift Configuration, AIAA J., Vol 43, No. 11, pp 2372-2384, 2005

[7] Schrijer F.F.J. & Scarano F. 2008. Effect of predictor–corrector filtering on the stability and spatial resolution of iterative PIV interrogation. *Exp Fluids* 45: 927-941.

[8] Schrijer F.F.J., Sciacchitano A. & Scarano F. 2014. Spatio-temporal and modal analysis of unsteady fluctuations in a high-subsonic base flow. *Phys. Fluids* 26: 086101.